

A reprint from

Optical Engineering

MARCH/APRIL 1978 17:2:170

ISSN 0036-1860

THE JOURNAL OF THE SOCIETY OF PHOTO-OPTICAL INSTRUMENTATION ENGINEERS

© 1978 by the Society of Photo-Optical Instrumentation Engineers
Box 10, Bellingham, Washington 98225 USA. Telephone 206/676-3290

HETERODYNE CORRELATION RADIOMETRY

Malvin Carl Teich

Columbia Radiation Laboratory
Columbia University
New York, New York 10027

Heterodyne Correlation Radiometry

Malvin Carl Teich

Columbia Radiation Laboratory
Columbia University
New York, New York 10027

Abstract

A heterodyne correlation radiometer is considered for the sensitive detection of radiating species whose Doppler shift is known, but whose presence we wish to affirm. Such radiation (which may be actively induced) can arise, for example, from remote molecular emitters, impurities and pollutants, trace minerals, chemical agents, or a general multiline source. A radiating sample of the species to be detected is physically made a part of the laboratory receiver, and serves as a kind of frequency-domain template with which the remote radiation is correlated, after heterodyne detection. The system is expected to be especially useful for the detection of sources whose radiated energy is distributed over a large number of lines, with frequencies that are not necessarily known. Requirements for local oscillator stability and tunability are less stringent than in the conventional heterodyne system and the use of a multiline local oscillator may be advantageous. It is shown that the minimum detectable power is expressible in a form similar to that for conventional heterodyning (for both quantum-noise-limited and Johnson-noise-limited detectors). The notable distinction is that the performance of the proposed system improves with increasing density of detected remotely radiating signal lines and increasing radiation power from the local sample. Performance degradation due to undesired impurity radiation is considered and shown to be tolerable in most cases. The technique should be applicable over a broad frequency range from the microwave to the optical, with its most likely use in the infrared.

I. Introduction

In a recent series of papers, three-frequency nonlinear heterodyne detection has been shown to be a useful technique for the acquisition of weak communications and radar signals in the presence of substantial Doppler shift.¹⁻⁴ The same concept has also been considered in the context of a multiple-frequency passive configuration, for the selective heterodyne detection of radiation from known remote species moving with unknown velocities.^{4,5} Basically, the system uses a nonlinear element to provide an output signal near a predetermined difference frequency f_c , which is independent of the Doppler shift of the received signals. The quantity f_c may be the frequency difference between two transmitter modes,^{1-4,6} or the rest difference frequency between two waves emitted from a remotely radiating molecule.^{4,5} The signal-to-noise ratio (SNR) obtainable with the nonlinear heterodyne system can be substantially higher than that obtainable with a conventional heterodyne system by virtue of the (often considerable) decrease in receiver bandwidth that is possible and the relatively small amount of receiver noise introduced by the nonlinear element.

This work was supported by the Joint Services Electronics Program under Contract No. DAAG29-77-C-0019.

Paper 1403 received September 15, 1976; revised September 1, 1977. A preliminary version of this work was presented at the Seminar on Unconventional Spectroscopy, SPIE Annual Meeting, San Diego, California, August 24-25, 1976, and appears in the Proceedings of that meeting, SPIE volume 82, pp. 132-145.

In this paper, we consider the use of the same principle in an altered configuration,⁷ to sensitively detect the signature of a (molecular) species whose Doppler feature is known, but whose presence we wish to affirm. A radiating sample of the species to be detected is physically made a part of the laboratory receiver, and serves as a kind of frequency-domain template with which the remote radiation is correlated, after heterodyne detection. The system will be especially useful for the detection of molecules whose radiated energy is distributed over a large number of lines, with frequencies that are not necessarily known. Examples include the radiation from complex molecules at submillimeter wavelengths and molecular radiation in the infrared and optical. We observe that remote conventional heterodyne radiometry and spectroscopy have recently begun to find use at these higher frequencies.⁸⁻¹² Detailed studies of the sensitivity limits of a real infrared heterodyne spectrometer for astrophysical use have been carried out by Abbas et al.¹² and by de Graauw.¹³ De Graauw also provides an interesting comparison between heterodyne spectrometry and other available methods. Indeed, attention has recently been drawn to a number of multiplexing or correlation techniques useful for increasing the detectability of a weak signal, including Fourier-transform spectrometry,¹⁴ gas-cell correlation spectrometry,¹⁵ and Fabry-Perot interferometry for periodic rotational Raman spectra.¹⁶ The system described here provides the advantages of heterodyning in conjunction with correlation.

II. System Configuration

A block diagram of the remote-detection version of the proposed system is illustrated in Figure 1. The remotely radiating

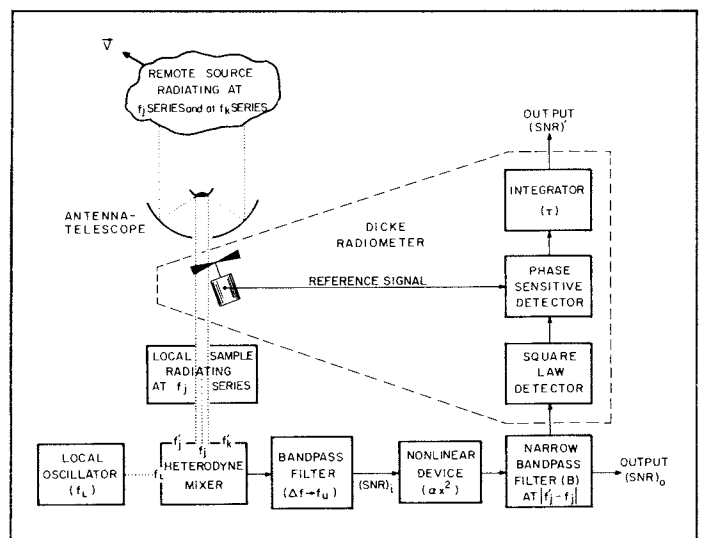


Figure 1. Block diagram for the heterodyne correlation radiometer. Dotted lines represent radiation signals, solid lines with arrows represent electrical signals, and dashed lines enclose one version of a Dicke radiometer that can be added to the system if required.

source emits electromagnetic radiation at a series J of rest signal frequencies f_j (j integer). Also present in the same source are other undesired species (impurities), emitting radiation at the series K of rest frequencies f_k (k integer). The f_j radiation, as well as the f_k radiation, will in general be Doppler shifted due to the mass motion (Doppler feature) of the source, and will arrive at the receiving station with frequencies f'_j and f'_k , respectively. These series are referred to as J' and K' . Assuming that the velocity of the cloud is much smaller than the speed of light c , the nonrelativistic Doppler formula provides

$$f'_j = f_j(1 \pm v_{||}/c) \quad (1a)$$

and

$$f'_k = f_k(1 \pm v_{||}/c) \quad (1b)$$

where $v_{||}$ is the radial component of the over-all velocity vector \vec{v} (see Figure 1). Individual lines will also be broadened, in general, due to the constituent particle velocity spectrum.

The received remote radiation is then combined with the radiation from a local sample of the species to be detected, which is at rest in the laboratory frame and therefore emits at frequencies f_j . The three series of frequencies (f'_j , f_j , and f'_k) are mixed in a heterodyne detector with a strong, coherent, and polarized local oscillator (LO) signal at frequency f_L to produce three series of strong electrical beat signals at $|f'_j - f_L|$, $|f_j - f_L|$, and $|f'_k - f_L|$, along with a dc component that is blocked. This is shown schematically in Figure 2. Signals at $|f'_j - f_j|$, $|f'_j - f'_k|$, and $|f_j - f'_k|$, arising without benefit of the LO, are

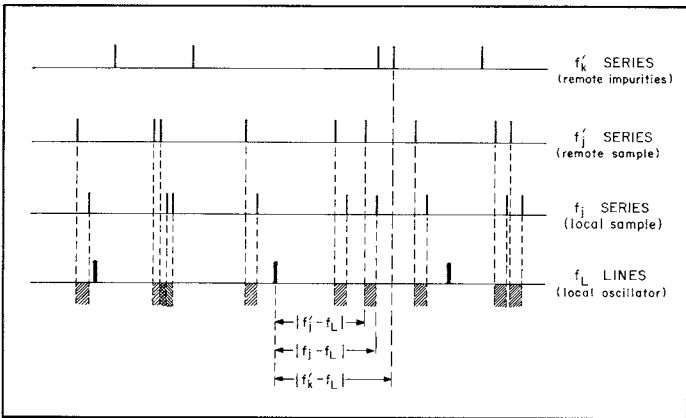


Figure 2. Schematic representation of frequency mixing in the heterodyne correlation radiometer. The cross-hatched areas represent individual line contributions (from line pairs j) to the over-all detected signal power. The technique is most useful for detecting species whose radiated energy is distributed over a large number of lines. Note that the frequencies f_j and f_L need not be known whereas the Doppler shift frequency $|f'_j - f_j|$ is assumed to be known *a priori*. The local oscillator may be multimode, non-stabilized, and non-tunable.

weak and may be neglected. In the infrared and optical, optimum mixing requires coincident, plane, parallel, and polarized waves normally incident on the photodetector;¹⁷ thus spatial first-order coherence is required over the detector aperture.¹⁸⁻²¹ As shown in Figure 1, the ac output of the heterodyne mixer must then be coupled, through a filter of bandwidth Δf , to a nonlinear (memoryless) device. Provided that the bandwidth Δf encompasses several lines produced by the species to be detected, its value is not critical as we shall see shortly. The nonlinear device, which is assumed to have a response over Δf , then generates a component of power at the Doppler shift frequency

$$|f'_j - f_j| = (v_{||}/c)f_j \quad (2)$$

for each j when both $|f'_j - f_L|$ and $|f_j - f_L|$ pass through Δf . Con-

tributions from individual values of j are shown as the cross-hatched areas in Figure 2. The greater the number n of these line pairs that pass through the filter, the greater the power generated at the Doppler shift frequency. It is also evident from Figure 2 that a multimode LO (indicated by 3 LO lines in our schematic) may increase the frequency range over which mixing occurs thereby increasing the likelihood that several lines are detected from the desired species.

Previous embodiments of the nonlinear heterodyne detection technique^{1,2} assumed that the Doppler shift (represented by $v_{||}$) was unknown within broad limits, but that the difference frequency f_c was known *a priori* to high accuracy. In the present circumstance, we assume that the radiated line frequencies are unknown but that the Doppler shift ($v_{||}$) is known *a priori*, at least to good approximation (see Figure 2). As previously,¹⁻⁶ the nonlinear device output is independent of LO frequency and amplitude fluctuations, within broad limits. (A careful choice of the LO frequency will often be useful, however.) A narrow-band filter centered at $|f'_j - f_j|$ and of bandwidth B , placed after the nonlinear device, achieves a low noise bandwidth (see Figure 1). Only the heterodyne mixer and the nonlinear device need have high-frequency response in many instances. Thus, amplifiers and other detection apparatus following the nonlinear device, though omitted in the block diagram for simplicity, process electrical signals at (usually) moderate frequencies, which provides ease of matching as well as good receiver noise figure. This, in turn, decreases the LO power necessary for optimum coherent detection.¹⁹⁻²¹ The effects of accidental contributions at $|f'_j - f_j|$ arising from the K' series can generally be neglected, as will be seen later.

If warranted, the output of the narrow bandpass filter may be fed into a standard Dicke radiometer^{22-24, 9-13} (dashed box in Figure 1) consisting of a (third) detector, a phase-sensitive (synchronous) detector, and an integrator with time constant τ . Although we specify that the third detector is square-law in Figure 1, its characteristic is not critical and, in fact, a linear detector will often provide the cleanest signal. The modulation may be obtained from a chopper as indicated in Figure 1, though in some circumstances it might be advantageous to switch the frequency of the narrow bandpass filter instead of the remote radiation (for baseline elimination). The use of a Dicke radiometer will generally provide improvement in the SNR and has been coupled with conventional infrared heterodyne systems in a number of instances.⁸⁻¹³ It may also be advantageous to use a balanced mixer in this configuration.^{8, 13}

III. Calculation of the Ideal SNR

The SNR at the output (o) of the heterodyne correlation radiometer $(SNR)_o$ is given by [see Eqs. (45) and (77) of Ref. 2, Part 1, and Eq. (4) of Ref. 5]

$$(SNR)_o = \rho \kappa (SNR)_i^2 / [1 + 2(SNR)_i] \quad (3)$$

assuming the use of a coherent LO that produces no excess noise, a bandpass filter close to low-pass ($\Delta f \rightarrow f_u$), and a square-law nonlinear device (for which it is easy to carry out the calculation). Here $(SNR)_i$ represents the SNR at the input (i) to the square-law device (see Figure 1) and will often be $\ll 1$. For the particular cases examined previously,¹⁻⁵ the constant ρ is bounded by $1 \leq \rho \leq 2$ for LO frequencies such that $f_L < f'_j, f_j$ or $f_L > f'_j, f_j$, which is the usual situation. Only in certain special cases does ρ exceed 2.^{5, 6}

For the multiple-frequency nonlinear heterodyne configurations considered earlier,¹⁻⁵ the quantity κ was shown to depend on the magnitude and on the statistical and spectral nature of the received radiation, as well as on the widths of the two bandpass filters. Calculations for κ have been carried out for the heterodyne correlation radiometer considered here (see Appendix A of Ref. 7), and the results turn out to be similar to those ob-

tained previously [see Eq. (5) of Ref. 5]. A number of specific cases are of interest: sinusoidal signals (s), independent Gaussian signals with Gaussian spectra (g), and independent Gaussian signals with Lorentzian spectra (ℓ). The Gaussian case is particularly important since radiation from astronomical sources is generally Gaussian.²⁵ For these cases, κ is given by (see Appendix A of Ref. 7)

$$\kappa_s \approx \frac{f_u}{B} \left[\frac{\sum_{j=1}^n A_j'^2 A_j^2}{\left\{ \sum_{j=1}^n [A_j'^2 + A_j^2] + \sum_{k=1}^m A_k'^2 \right\}^2} \right], \quad (4a)$$

$$\kappa_g \approx \frac{f_u}{\sqrt{8}\gamma} \left[\frac{\sum_{j=1}^n (\gamma P_j') (\gamma P_j)}{\left\{ \sum_{j=1}^n [\gamma P_j' + \gamma P_j] + \sum_{k=1}^m \gamma P_k' \right\}^2} \right] \times \left(\frac{2\Phi(B/\sqrt{8}\gamma) - 1}{(B/\sqrt{8}\gamma)} \right), \quad (4b)$$

and

$$\kappa_\ell \approx \frac{f_u}{2\Gamma} \left[\frac{\sum_{j=1}^n D_j' D_j}{\left\{ \sum_{j=1}^n [D_j' + D_j] + \sum_{k=1}^m D_k' \right\}^2} \right] \times \left(\frac{\pi^{-1} \tan^{-1} \left\{ (2B/\Gamma) [4 - (B^2/4\Gamma^2)]^{-1} \right\}}{B/2\Gamma} \right). \quad (4c)$$

Here, A_j (A_j', A_k') represents the amplitude of the j th (f_j' th, f_k' th) line in the sinusoidal case, P_j (P_j', P_k') represents the peak value of the Gaussian spectral distribution, and γ is its standard deviation, whereas D_j (D_j', D_k') and Γ represent the height and width of the Lorentzian spectrum, respectively. The index j ranges from 1 through n , representing the n line pairs permitted through the bandpass filter $\Delta f = f_u$, after mixing with the LO. Similarly, k ranges from 1 through m . The quantity Φ is the error function. It has been assumed for simplicity that all spectral widths are identical, i.e., $\gamma_j' = \gamma_j = \gamma_{j+1}' = \gamma_{j+1} = \gamma_k' \equiv \gamma$ and $\Gamma_j' = \Gamma_j = \Gamma_{j+1}' = \Gamma_{j+1} = \Gamma_k' \equiv \Gamma$; similar but more complex expressions are obtained when this is not the case.

For quantum-noise-limited detectors such as photoemitters and reverse-biased photodiodes operating in the infrared and optical, assuming that the incident radiation and the coherent LO are plane parallel waves with the same axis of polarization, the ideal input SNR to the nonlinear device is^{18-21, 26}

$$(SNR)_i = \eta P_r / h\nu f_u, \quad h\nu \gg kT. \quad (5)$$

Here η is the detector quantum efficiency, $h\nu$ is the photon energy, kT is the thermal excitation energy (k is Boltzmann's constant and T is the detector temperature), and P_r is defined as the total received signal radiation power, i.e.,

$$P_r = \sum_{j=1}^n [P_{0j}' + P_{0j}] + \sum_{k=1}^m P_{0k}'. \quad (6)$$

The symbol P_{0j} represents the power in the j th line; thus for the

sinusoidal case $P_{0j} = \frac{1}{2} A_j^2$, for the Gaussian/Gaussian case $P_{0j} = 2\sqrt{2\pi} \gamma P_j$, and for the Gaussian/Lorentzian case $P_{0j} = \pi D_j$. For photovoltaic detectors (e.g., HgCdTe or PbSnTe) and photoconductive detectors (e.g., Ge:Cu or Ge:Au), the input SNR is generally one-half that given in Eq. (5) as a result of additional generation-recombination (g-r) noise.¹⁹⁻²¹

Heterodyne detectors in the microwave and millimeter-wave regions ($h\nu \ll kT$) include square-law mixers such as the crystal diode detector,²⁷ the InSb photoconductive detector,²⁸⁻³⁰ the Golay cell,²⁹ the pyroelectric detector,²⁹ the metal-oxide-metal diode, and the bolometer.²⁴ The latter three types of detectors have also been used successfully in the middle infrared (at 10.6 μ m).³¹⁻³⁴ Of particular interest in the millimeter and far-infrared regions are the low-noise fast Schottky-barrier diodes recently used in a number of experiments for astronomical observations.^{30, 35, 36} For this type of detector Johnson noise generally predominates, and the input SNR is given by³⁴

$$(SNR)_i = P_r / kT F_T f_u = P_r / kT_{eff} f_u \quad (7)$$

For simplicity, we have lumped a number of detector parameters and operating conditions in the receiver noise figure F_T and in the receiver effective temperature T_{eff} .

Thus, the output SNR is obtained by choosing a value of ρ and combining Eqs. (3)-(7). A number of further simplifying assumptions are possible, however, and we consider these in the next section.

IV. Further Approximations for the SNR and the MDP

We now consider the plausible case where each and every locally produced line f_j , and its corresponding detected signal line f_j' maintain a constant power ratio defined as ζ . Thus,

$$\zeta(s) \equiv A_j^2 / A_j'^2 = A_{j+1}^2 / A_{j+1}'^2, \quad (8a)$$

$$\zeta(g) \equiv \gamma P_j / \gamma P_j' = \gamma P_{j+1} / \gamma P_{j+1}', \quad (8b)$$

and

$$\zeta(\ell) \equiv D_j / D_j' = D_{j+1} / D_{j+1}', \quad (8c)$$

so that the expressions in large square brackets in Eq. (4) become

$$\left[\dots \right]_{s,g,\ell} = \left[\frac{\zeta \sum_{j=1}^n P_{0j}'^2}{\left\{ (1+\zeta) \sum_{j=1}^n P_{0j}' + \sum_{k=1}^m P_{0k}' \right\}^2} \right] = \left[\frac{\zeta n \overline{P_0}'^2}{\left\{ (1+\zeta) n \overline{P_0}' + m \overline{P_0}' \right\}^2} \right] = \frac{1}{n} \left[\frac{\zeta}{(1+\zeta)^2} \right] \times \left(\frac{\overline{P_0}'^2}{\overline{P_0}'^2} \right) \left(1 + \frac{1}{(1+\zeta)} \frac{m \overline{P_0}'}{n \overline{P_0}'} \right)^{-2}. \quad (9)$$

Here, $\overline{P_0}'$ and $\overline{P_0}'^2$ represent the mean and mean-squared signal line power detected, respectively, and $\overline{P_0}'$ represents the mean impurity line power detected. For a single signal line ($n=1$) and no impurity radiation ($m=0$), Eq. (9) reduces to $\zeta(1+\zeta)^{-2}$ which, for $\zeta=1$, is equal to 1/4. This result is the same as that provided by Eq. (9) of Ref. 5 as it should be.

Inasmuch as the quantities in large round parentheses in Eqs. (4b) and (4c) are of order unity for $B \lesssim \gamma(\Gamma)$, it is the larger of

B and $\gamma(\Gamma)$ which limits κ and therefore the SNR in the Gaussian signal case. For instance, inspection of Eq. (4b) shows that for very large γ the numerator of the fraction in large round parentheses becomes small whereas very large B yields a large denominator. Either effect clearly reduces κ . As an example for the Gaussian spectrum case with $B = \sqrt{8} \gamma$, $[2\Phi(1)-1] = 0.68$ whereas for the Lorentzian spectrum case with $B = 4(\sqrt{2}-1)\Gamma \approx 1.66\Gamma$, $\pi^{-1} \tan^{-1} 1 = 1/4$. Thus the SNRs for the Gaussian and Lorentzian cases are reduced below that for the sinewave case (delta-function spectrum) for the same bandwidth B. This is understood to arise from the fact that some signal is being excluded in the Gaussian and Lorentzian cases in comparison with the delta-function case, but the noise is approximately the same. For fixed $\gamma(\Gamma)$, the best SNR for the Gaussian and Lorentzian cases is obtained as $B \rightarrow 0$, since the noise decreases faster than the signal, as B decreases, assuming that all of the center frequencies $|f_j - f_j|$ precisely coincide. In actuality, however, the center frequencies are spread over the range $(v_{||}/c)|f_n - f_1| \lesssim (v_{||}/c)f_u$, and it is therefore not generally helpful to decrease B below this value. Small B does, however, provide a minor advantage in minimizing false signals from the K series, as we will see later.

For $B \gg \gamma(\Gamma)$, essentially all of the signal is included, and the results reduce to those obtained in the sinewave case. All other things being equal, then, these considerations dictate choosing lines for which the (Doppler) widths and, less importantly, the bandpass f_u are minimized. Nevertheless, f_u should be sufficiently large to insure that several line pairs will be passed through the bandpass filter so that $\overline{P_0'^2}$ and $\overline{P_0'}$ will indeed benefit from the indicated averaging. Large f_u , furthermore, provides small (SNR)_i and a simple expression for (SNR)_o, as discussed in Section V. As we will see shortly, system performance in fact depends on the quantity f_u/n rather than on f_u directly, so that the value chosen for f_u is reasonably arbitrary for a relatively dense population of lines.

The total received radiation power expressed in Eq. (6) may also be rewritten in terms of the ratio ζ to provide

$$P_T = (1+\zeta)n\overline{P_0'} \left(1 + \frac{1}{(1+\zeta)} \frac{m\overline{P_0'}}{n\overline{P_0'}} \right) \quad (10)$$

For clarity, we now provide an explicit expression for (SNR)_o in the case of a Gaussian/Gaussian signal with the conditions and approximations expressed above. We conservatively choose $\rho \approx 1$ and consider a quantum-noise-limited detector. Using Eqs. (3), (4b), (5), (8b), (9), and (10), we obtain

$$\begin{aligned} (\text{SNR})_o \approx & \frac{\eta^2 \zeta n \overline{P_0'^2} / \sqrt{8} \gamma f_u h^2 \nu^2}{1 + \left[\frac{2\eta(1+\zeta)n\overline{P_0'}}{h\nu f_u} \right] \left[1 + \frac{1}{(1+\zeta)} \frac{m\overline{P_0'}}{n\overline{P_0'}} \right]} \\ & \times \left(\frac{2\Phi(B/\sqrt{8}\gamma) - 1}{(B/\sqrt{8}\gamma)} \right) \quad (11) \end{aligned}$$

Further simplification occurs for the usual case when $B \lesssim \gamma$, whereupon the quantity in large round parentheses above is about 4/5. Finally, we make the assumption that (SNR)_i \ll 1, implying that signal-by-noise ($s \times n$) terms are small in comparison with noise-by-noise ($n \times n$) terms. This is a reasonable assumption for weak signals and for calculations of the minimum detectable power (MDP), and has the effect of making the denominator of Eq. (3) equal to unity. Incorporating these additional approximations in Eq. (11) provides the much simplified expression

$$(\text{SNR})_o \approx \frac{\sqrt{2} \eta^2 \zeta n \overline{P_0'^2}}{5\gamma f_u h^2 \nu^2} \quad (12)$$

The minimum detectable rms line power (MDP)_o, at the output of the system, is obtained by setting (SNR)_o = 1 in Eq. (12) and solving for $[\overline{P_0'^2}]^{1/2}$. This yields

$$(\text{MDP})_o \approx \frac{h\nu}{\eta} \left(\frac{5\gamma f_u}{\sqrt{2}\zeta n} \right)^{1/2} \quad (13a)$$

for quantum-noise-limited detection. Similarly, using Eq. (7) for Johnson-noise-limited detection in place of Eq. (5), we obtain

$$(\text{MDP})_o \approx kT_{\text{eff}} \left(\frac{5\gamma f_u}{\sqrt{2}\zeta n} \right)^{1/2} \quad (13b)$$

The substantive difference between Eqs. (13a) and (13b) here and Eqs. (13a) and (13b) of Ref. 5 lies in the presence of the factor ζn ; system detectability is seen to improve with increasing ζ and increasing n in the bandpass f_u . Of course, lines are counted only if both the remote and local samples contribute at a particular frequency. Defining $\bar{f} \equiv f_u/n$ as the mean frequency interval between signal lines in the species whose presence we wish to affirm, and $\bar{\gamma}$ as the average linewidth, Eq. (13) may be rewritten as

$$(\text{MDP})_o \approx 2 \frac{h\nu}{\eta} \sqrt{\bar{\gamma}\bar{f}/\zeta} \quad (14a)$$

for quantum-noise-limited detection, and as

$$(\text{MDP})_o \approx 2kT_{\text{eff}} \sqrt{\bar{\gamma}\bar{f}/\zeta} \quad (14b)$$

for Johnson-noise-limited detection. For simplicity, we have taken $(5/\sqrt{2})^{1/2} = 1.8803 \approx 2$ in Eq. (14). This expression represents the minimum average line radiation power required to be received for definitive detection. It indicates that small $\bar{\gamma}$ and \bar{f} , and large ζ are desired, and that \bar{f} rather than f_u is the important parameter, as indicated earlier. Thus, it will be easiest to detect a substance whose spectrum consists of a dense series of narrow lines that can also be made to radiate high power locally. For $B \gg \bar{\gamma}$, $2\bar{\gamma}^{1/2}$ must be replaced by $B^{1/2}$ in Eq. (14). We recall that it is not generally helpful to decrease B below $(v_{||}/c)f_u$, which is the center frequency spread. In a real system, furthermore, the sensitivity will be degraded below the ideal limits set forth above.¹²

V. Correction Factors for Impurity Species

The deleterious effect of the impurity frequency series K on the SNR and MDP arises from both the $s \times s$ (signal-by-signal) and the $s \times n$ contributions to the output power spectral density. The calculation for the latter is straightforward and has been included in Eq. (3), through the factor $[1+2(\text{SNR})_i]$ in the denominator. For small values of (SNR)_i, it is intuitively clear that the $n \times n$ contributions outweigh the $s \times n$ contributions, and the approximation following Eq. (11) suffices. The $s \times s$ contribution, on the other hand, arises from two distinct effects. The first represents the accidental occurrence of an f'_k line in a band of width B about an f_j or an f'_j line thereby mixing with this companion signal line to provide a false $s \times s$ component (see Figure 2).

If we assume that both the f'_j and the f'_k lines are Poisson distributed in frequency, with rate parameters a and b respectively, an order-of-magnitude estimate for the average power in the $s \times s$ component due to this effect is proportional to $4(1+\zeta)nbB\overline{P_0'}\overline{P_0'}$ (see Appendix B of Ref. 7). Comparison with the true signal $s \times s$ contribution whose output power is proportional to $\zeta n \overline{P_0'^2}$ as given in Eq. (9), demonstrates that, at least for $\overline{P_0'} \sim \overline{P_0'}$, the correction factor may be ignored in the usual situation when $bB \ll 1$ and $\zeta \gtrsim 1$. If these conditions are not fulfilled, and/or if $\overline{P_0'} \gg \overline{P_0'}$, the correction must be applied,

in which case this signal must be considered as a noise pedestal due to accidental coincidences and therefore subtracted from the measured signal. There are, however, accidental true signal contributions that reduce this deleterious effect (see Appendix B of Ref. 7).

The second impurity effect contributing to the $s \times s$ term arises from frequency differences of lines in the K series that accidentally fall at $|f'_i - f_j|$. Again making use of the Poisson assumption for the frequency distribution of the f_k lines, it follows that the inter-frequency spacing distribution $p(f)$ is gamma distributed in general, and for adjacent lines is exponentially distributed as $\text{bexp}(-bf)$ for $f \geq 0$. An estimate for the number of lines detected at such an accidental frequency separation, within B Hz of $|f'_i - f_j|$, is $< mbB$ (see Appendix B of Ref. 7). The correction factor for the power, using the same proportionality constant as above, in this case is $< mbB P_0^2$ which can be of the same order of magnitude as the correction factor due to accidental coincidences. In many cases of practical interest, therefore, the previously presented results may be used without correction for impurity species.

VI. Discussion

A heterodyne correlation radiometer has been described for the sensitive detection of local and remote species such as pollutants, interstellar molecules, and trace minerals. It can also be used to distinguish between isotopes. The system operates on the basis of the fixed difference frequencies between the emission lines of a weak remote species and a locally radiating sample of that species. It introduces little loss over the conventional heterodyne radiometer and can often provide a decreased noise bandwidth as well as a number of other specific advantages. The technique generally requires knowledge only of the Doppler shift of the remotely radiating source and not of its emission frequencies, which are sometimes unknown or difficult to determine.³⁷ It does not require a stabilized LO, though tunability can be useful in maximizing the remote power detected. High-frequency response is demanded only of the heterodyne mixer and the nonlinear device; subsequent electrical signals are generated at (usually) moderate frequencies providing ease of matching, good receiver noise figure, and modest requirements for LO power. The technique is expected to be especially useful for the detection of remote or local species whose radiated energy is distributed over a large number of lines.

The ideal SNR and MDP at the output of the system have been obtained for a number of cases of interest, including sinusoidal signals and Gaussian signals with both Gaussian and Lorentzian spectra. Small linewidths and closely spaced lines are seen to enhance detectability, as does a strongly radiating local sample. Of course, the remote source should be as strong as possible for definitive detection. Correction factors for impurity species have been accounted for and are not expected to seriously impair operation of the system. For certain choices of parameters, the SNR at the output of the heterodyne correlation radiometer will provide a sufficient confidence level for detection. For situations in which this is not the case, further improvement can be obtained by using a classical radiometer, a balanced mixer, and/or a multichannel receiver. If the Doppler shift is unknown, for example, a multichannel receiver using a bank of narrow bandwidth filters can replace the single narrow bandpass filter (B), thereby substantially compressing the number of channels below that required in the conventional system. For the detection of multiline radiation from astronomical sources, the real SNR will be reduced by a variety of deleterious effects in analogy with the conventional system.¹²

The technique should operate over a broad frequency range from the microwave to the optical. For the detection of astronomical radiation, a possible candidate is the infrared emission from CO which exists in relatively high densities and with a very broad range of velocities in interstellar regions, as determined

by its millimeter-wave emission.^{38, 39} Clearly, the same considerations apply to the detection of multiple-line maser radiation from astronomical sources,⁴⁰⁻⁴³ and to the detection of remote pollutants.^{44, 45} The technique can only be used for sufficiently nonreactive substances that emit in the terrestrial laboratory as well as remotely, thus excluding, for example, CN^{46} and C_2H^{47} . Again we note that spectroscopic information about a molecule is not provided.

For the submillimeter region, it may be possible to use a combination Schottky-barrier-diode/harmonic-mixer that would provide an output at low frequencies as long as the high-frequency beat signals are generated and mixed within the detector. LO harmonics are also readily generated in these devices³⁵ so that harmonic-mixing heterodyne correlation radiometry could be performed.⁴⁸ Josephson junctions, which can sometimes be made to produce their own LO power,³⁰ and metal-oxide-metal diodes could also be used. An IMPATT solid-state oscillator could conveniently be considered as an LO in these regions since frequency stabilization, which is difficult to achieve in these devices,³⁰ is not required. At higher frequencies, tunable diode lasers and Schottky-barrier detectors may be useful components.

Acknowledgment

It is a pleasure to thank Patrick Thaddeus for valuable discussions. I am grateful to Richard Meyers for critically reading the manuscript and for verifying many of the results.

References

1. M. C. Teich, *Appl. Phys. Lett.* **15**, 420 (1969).
2. M. C. Teich and R. Y. Yen, *Appl. Opt.* **14**, 666 (1975); **14**, 680 (1975).
3. M. C. Teich, U. S. Patent No. 3,875,399 (1975).
4. M. C. Teich, "Nonlinear Heterodyne Detection," in *Topics in Applied Physics*, edited by R. J. Keyes (Springer-Verlag, New York, 1977), vol. 19, *Optical and Infrared Detectors*, ch. 7.
5. M. C. Teich, *Rev. Sci. Instr.* **46**, 1313 (1975).
6. R. L. Abrams and R. C. White, Jr., *IEEE J. Quantum Electron.* **QE-8**, 13 (1972).
7. M. C. Teich, *Proc. Soc. Photo-Opt. Instr. Eng.* **82**, 132 (1976).
8. T. de Graauw and H. van de Stadt, *Nature (London) Phys. Sci.* **246**, 73 (1973); H. van de Stadt, *Astron. Astrophys.* **36**, 341 (1974).
9. J. Gay, A. Journet, B. Christophe, and M. Robert, *Appl. Phys. Lett.* **22**, 448 (1973); D. DeBatz, P. Granes, J. Gay, and A. Journet, *Nature (London) Phys. Sci.* **245**, 89 (1973).
10. D. W. Peterson, M. A. Johnson, and A. L. Betz, *Nature (London) Phys. Sci.* **250**, 128 (1974); A. L. Betz, M. A. Johnson, R. A. McLaren, and E. C. Sutton, *Astrophys. J.* **208**, L141 (1976); M. A. Johnson, A. L. Betz, R. A. McLaren, E. C. Sutton, and C. H. Townes, *Astrophys. J.* **208**, L145 (1976).
11. M. A. Frerking and D. J. Muehler, *Appl. Opt.* **16**, 526 (1977).
12. M. M. Abbas, M. J. Mumma, T. Kostiuik, and D. Buhl, *Appl. Opt.* **15**, 427 (1976).
13. T. de Graauw, "Infrared Heterodyne Detection in Astronomy: Experiments and Observations," Doctoral Dissertation, University of Utrecht (1975).
14. P. B. Felgett, *J. Phys. Rad.* **19**, 187 (1958).
15. K. F. Luft, *J. Tech. Phys.* **24**, 97 (1943); T. V. Ward and H. H. Zwick, *Appl. Opt.* **14**, 2896 (1975); R. T. Menzies, NASA Tech Brief B75-10275, October 1975.
16. J. J. Barrett and S. A. Meyers, *J. Opt. Soc. Am.* **61**, 1246 (1971); J. J. Barrett, *Opt. Eng.* **16**, 85 (1977).
17. A. E. Siegman, *Proc. IEEE* **54**, 1350 (1966).
18. M. C. Teich, *Appl. Phys. Lett.* **14**, 201 (1969); "Quantum Theory of Heterodyne Detection," in *Proc. Third Photocond. Conf.*, edited by E. M. Pell (Pergamon, New York, 1971), pp. 1-5.
19. M. C. Teich, R. J. Keyes, and R. H. Kingston, *Appl. Phys. Lett.* **9**, 357 (1966).
20. M. C. Teich, *Proc. IEEE* **56**, 37 (1968); **57**, 786 (1969).
21. M. C. Teich, "Coherent Detection in the Infrared," in *Semiconductors and Semimetals*, edited by R. K. Willardson and A. C. Beer (Academic, New York, 1970), vol. 5, *Infrared Detectors*, ch. 9.
22. R. H. Dicke, *Rev. Sci. Instrum.* **17**, 268 (1946).
23. J. D. Kraus, *Radio Astronomy* (McGraw-Hill, New York, 1966).
24. T. G. Phillips and K. B. Jefferts, *IEEE Trans. Microwave Theory Tech.* **MTT-22**, 1290 (1974).
25. N. J. Evans II, R. E. Hills, O. E. H. Rydbeck, and E. Kollberg, *Phys. Rev. A* **6**, 1643 (1972).

26. M. C. Teich and R. Y. Yen, *J. Appl. Phys.* *43*, 2480 (1972).
 27. C. H. Townes and A. L. Schawlow, *Microwave Spectroscopy* (McGraw-Hill, New York, 1955).
 28. E. H. Putley, *Proc. IEEE* *54*, 1096 (1966).
 29. H. A. Gebbie, N. W. B. Stone, E. H. Putley, and N. Shaw, *Nature (London) Phys. Sci.* *214*, 165 (1967).
 30. A. A. Penzias and C. A. Burrus, *Ann. Rev. Astron. Astrophys.* *11*, 51 (1973).
 31. R. L. Abrams and A. M. Glass, *Appl. Phys. Lett.* *15*, 251 (1969).
 32. E. Leiba, *C. R. Acad. Sci. B* *268*, 31 (1969).
 33. R. L. Abrams and W. B. Gandrud, *Appl. Phys. Lett.* *17*, 150 (1970).
 34. B. Contreras and O. L. Gaddy, *Appl. Phys. Lett.* *18*, 277 (1971).
 35. H. R. Fetterman, B. J. Clifton, P. E. Tannenwald, C. D. Parker, and H. Penfield, *IEEE Trans. Microwave Theory Tech.* *MTT-22*, 1013 (1974).
 36. K. Mizuno, R. Kuwahara, and S. Ono, *Appl. Phys. Lett.* *26*, 605 (1975).
 37. B. Zuckerman and P. Palmer, *Ann. Rev. Astron. Astrophys.* *12*, 279 (1974).
 38. R. W. Wilson, K. B. Jefferts, and A. A. Penzias, *Astrophys. J.* *161*, L43 (1970).
 39. P. M. Solomon, *Phys. Today* *26*(3), 32 (1973).
 40. D. M. Rank, C. H. Townes, and W. J. Welch, *Science* *174*, 1083 (1971).
 41. M. M. Litvak, *Ann. Rev. Astron. Astrophys.* *12*, 97 (1974).
 42. L. E. Snyder and D. Buhl, *Astrophys. J.* *189*, L31 (1974).
 43. L. E. Snyder, *IEEE Trans. Microwave Theory Tech.* *MTT-22*, 1299 (1974).
 44. E. D. Hinkley and P. L. Kelley, *Science* *171*, 635 (1971).
 45. R. Menzies, *Appl. Phys. Lett.* *22*, 592 (1973).
 46. A. A. Penzias, R. W. Wilson, and K. B. Jefferts, *Phys. Rev. Lett.* *32*, 701 (1974).
 47. K. D. Tucker, M. L. Kutner, and P. Thaddeus, *Astrophys. J.* *193*, L115 (1974).
 48. P. F. Goldsmith, R. L. Plambeck, and R. Y. Chiao, *IEEE Trans. Microwave Theory Tech.* *MTT-22*, 1115 (1974). ☉
-